FGF signal-dependent segregation of primitive endoderm and epiblast in the mouse blastocyst

Yojiro Yamanaka[1,*,†,‡], Fredrik Lanner[1,*] and Janet Rossant[1,2,‡]

SUMMARY

Primitive endoderm (PE) and epiblast (EPI) are two lineages derived from the inner cell mass (ICM) of the E3.5 blastocyst. Recent studies showed that EPI and PE progenitors expressing the lineage-specific transcriptional factors Nanog and Gata6, respectively, arise progressively as the ICM develops. Subsequent sorting of the two progenitors during blastocyst maturation results in the formation of morphologically distinct EPI and PE layers at E4.5. It is, however, unknown how the initial differences between the two populations become established in the E3.5 blastocyst. Because the ICM cells are derived from two distinct rounds of polarized cell divisions during cleavage, a possible role for cell lineage history in promoting EPI versus PE fate has been proposed. We followed cell lineage from the eight-cell stage by live cell tracing and could find no clear linkage between developmental history of individual ICM cells and later cell fate. However, modulating FGF signaling levels by inhibition of the receptor/MAP kinase pathway or by addition of exogenous FGF shifted the fate of ICM cells to become either EPI or PE, respectively. Nanog- or Gata6-expressing progenitors could still be shifted towards the alternative fate by modulating FGF signaling during blastocyst maturation, suggesting that the ICM progenitors are not fully committed to their final fate at the time that initial segregation of gene expression occurs. In conclusion, we propose a model in which stochastic and progressive specification of EPI and PE lineages occurs during maturation of the blastocyst in an FGF/MAP kinase signal-dependent manner.

KEY WORDS: ICM, Asymmetric division, Primitive endoderm, Epiblast, Nanog, Gata6, Mouse

INTRODUCTION

Primitive endoderm (PE) and epiblast (EPI) lineages form two distinct layers in the E4.5 implanting mouse embryo that are both derived from the inner cell mass (ICM) of the E3.5 blastocyst. The PE is an extraembryonic cell lineage, which gives rise primarily to visceral and parietal endoderm of the yolk sacs after implantation (Gardner, 1982; Gardner, 1984; Gardner and Rossant, 1979; Plusa et al., 2008). The EPI gives rise to the fetus and some of the extraembryonic tissues, such as amnion and extraembryonic mesoderm (Gardner and Papaioannou, 1975; Gardner and Rossant, 1979). The interactions between these two lineages in early postimplantation development are important not only to supply nutrients to the embryo, but also to establish anteroposterior polarity prior to gastrulation (Rossant and Tam, 2009).

In the blastocyst at E3.5, ICM cells appear morphologically as a homogeneous cell population, suggestive of bipotential cells generating both PE and EPI. The PE only emerges as a distinct monolayer on the surface of the ICM by implantation at E4.5. PE and EPI cells at this stage are lineage restricted, as they contribute only to their respective lineages in chimeric embryos (Gardner, 1982; Gardner, 1984; Gardner and Rossant, 1979). It was proposed that cell position in the ICM controlled segregation of the two lineages

(Rossant, 1975), with ICM cells directly facing the blastocoel becoming the PE and those embedded inside the ICM becoming the EPI. However, our previous study and subsequent studies by others suggested that the ICM of the fully expanded E3.5 blastocyst is not a homogeneous population but rather a mixed population of PE and EPI progenitors (Chazaud et al., 2006; Kurimoto et al., 2006; Plusa et al., 2008). Lineage tracing revealed that the fate of single E3.5 ICM cells was to form either the PE or the EPI, and rarely both. In addition, the lineage-specific markers Gata6 and Nanog were mutually exclusively expressed in the E3.5 ICM (Chazaud et al., 2006). Single cell cDNA expression analysis provided further evidence of heterogeneity in global gene expression among ICM cells (Kurimoto et al., 2006). Furthermore, live imaging analysis using the $Pdgfra^{H2B-GFP}$ mouse line, in which the PE is specifically labeled with histone H2B-GFP, generally supported the mosaic model but revealed that separation of the two lineages during blastocoel expansion involved both apoptosis and cell migration (Plusa et al., 2008). This study also showed that there was progressive mutual exclusion of Nanog and Gata6 expression in ICM cells during this stage from initial uniform co-expression in the early blastocyst (Plusa et al., 2008).

The mosaic/cell sorting model of EPI/PE formation requires that heterogeneity be generated in an apparently homogeneous population in a position-independent manner. One attractive model to explain this relies on the understanding of the process of inner cell generation during cleavage gained from studies using isolated blastomeres in the 1980s (reviewed by Johnson et al., 1986). These studies suggested that inner cells that give rise to the ICM are generated from two rounds of asymmetric divisions at the 8-16 and 16-32 cell stage. We previously proposed a model in which the developmental origins of individual ICM cells may relate to their later cell fate: inner cells generated in the first round of divisions (primary inner cells) have a preference to become the EPI, whereas cells generated in the second round (secondary inner cells) have a preference to become the PE

[1]Program in Developmental and Stem Cell Biology, Hospital for Sick Children Research Institute, Toronto, Ontario M5G 1X8, Canada. [2]Department of Molecular Genetics, University of Toronto, Toronto, Ontario M5G 1X8, Canada.

*These authors contributed equally to this work
†Present address: Rosalind and Morris Goodman Cancer Center, Department of Human Genetics, Faculty of Medicine, McGill University, Montreal, Quebec H3A 1A3, Canada
‡Authors for correspondence (janet.rossant@sickkids.ca; yojiro.yamanaka@mcgill.ca)

(Yamanaka et al., 2006) (see also Chisholm and Houliston, 1987). The idea behind this model is that the PE and the trophectoderm (TE), the outer cell layer of the blastocyst, are both extraembryonic lineages and share similar epigenetic characteristics; for example, paternal X inactivation (reviewed by Avner and Heard, 2001). Therefore, they may share a developmental origin as well. Primary inner cells would be set aside from the outer environment one cell cycle earlier than secondary inner cells and would be protected from taking up extraembryonic character, perhaps by the Hippo signaling pathway that is active in inside cells (Nishioka et al., 2009). Secondary inner cells would be predisposed by prolonged external position to become extraembryonic primitive endoderm once enclosed in the blastocyst (Yamanaka et al., 2006). This model is clearly testable by lineage tracing experiments.

Whether lineage history is important or not, there still needs to be some molecular pathway that initiates the differences between EPI and PE progenitors. A number of pieces of evidence suggest that the FGF/MAP kinase signal pathway might play this key role. Homozygous mutants of *Fgf4*, *Fgfr2* and *Grb2* all show peri-implantation lethality and complete lack of PE formation in vivo and in blastocyst outgrowths (Arman et al., 1998; Cheng et al., 1998; Feldman et al., 1995; Goldin and Papaioannou, 2003). Importantly, we have shown that the lack of the PE in the *Grb2* mutant blastocyst is due to the transformation of all ICM cells to the EPI fate, rather than to selective apoptosis or overproliferation of one lineage (Chazaud et al., 2006). Overexpression of a dominant-negative FGF receptor in ES cells blocks PE formation in embryoid bodies (EBs) in vitro (Chen et al., 2000), although exogenous FGF does not enhance PE differentiation in ES cells (Hamazaki et al., 2006). Treatment with a PTPase inhibitor, sodium vanadate, enhances PE differentiation, and ectopic expression of constitutively active MAPK/ERK kinase (MEK) initiates PE differentiation without EB formation (Hamazaki et al., 2006). Exogenous FGF treatment of preimplantation embryos showed increased cell numbers during blastocyst outgrowth, but their lineage identity was undefined (Rappolee et al., 1994).

In this study, we explore further the mechanisms driving PE and EPI specification. First, we examined whether the developmental origins of ICM cells relate to later cell fate. Using a live imaging technique, we traced the lineages of the ICM from the eight-cell stage and showed that both primary and secondary inner cells could contribute to EPI or PE at the postimplantation stage, with no apparent bias related to their origin, thus showing that the process of forming a primary or secondary inner cell is not sufficient to direct cell fate. We then examined the temporal requirement for activation of the FGF/MAP kinase signal for PE formation. We showed that modulating FGF signaling levels by either inhibition of the receptor/MAP kinase pathway or addition of exogenous FGF shifts the fate of ICM cells to become either Nanog-expressing or Gata6-expressing progenitors, respectively. Furthermore, although the progenitors in the E3.5 ICM express either Nanog or Gata6, their cell fate is still controlled by FGF signaling during blastocyst maturation. We showed that cell fate can still be altered by altering FGF signaling during blastocyst maturation. Taking these results together, we propose a model in which stochastic and progressive specification of EPI and PE lineages occurs during maturation of the blastocyst in an FGF/MAP kinase signal-dependent manner.

MATERIALS AND METHODS

Mouse embryos and in vitro culture condition
We used the ICR outbred mice maintained in 12-hour light cycle condition. Estrous females were crossed with ICR males, Z/EG (homozygous or heterozygous) males or *Pdgfra^H2B-GFP* heterozygous males. Cleavage-stage embryos were collected by flushing oviducts with M2 media (Chemicon). Embryos were cultured in KSOM (Chemicon) at 37°C, 6% CO_2. The inhibitor treatment was performed in wells of four-well dishes (Nunc) without a covering of mineral oil. The concentration of inhibitors we used were: FGF receptor inhibitor PD173074, 100 nM (Stemgent); Mek inhibitor PD0325901, 0.5 μM (Stemgent). For exogenous Fgf4 treatment, we used various doses of Fgf4 (7-1000 ng/ml, R&D Systems) with heparin (1 μg/ml) in KSOM. Embryos with/without the zona pellucida were cultured in microdrops (15 embryos/15 μl drop) covered with mineral oil. We confirmed that the presence of the zona pellucida did not change the exogenous FGF effects.

Immunostaining of preimplantation embryos
Embryos were collected from oviducts or uteri and fixed in 4% formaldehyde solution in PBS (Polysciences Inc.) for 15 minutes at room temperature. They were washed in PBT (PBS with 0.1% Tween 20) and permeabilized with 0.2% Triton in PBS for 15 minutes. The embryos were treated with primary antibodies overnight at 4°C after blocking in PBT with 5% FBS for at least 1 hour at room temperature. Primary antibodies used in this study were: Cdx2 (BioGenex, MU392-UC), Oct4 (Santa Cruz, C-10), Nanog (Cosmo Bio, REC-RCAB0002), Gata6 (R&D Systems, AF1700), Par6 (Abcam, ab45394) and Gata4 (Santa Cruz, H112). The embryos were then treated with secondary antibodies conjugated with Alexa Fluor 488, Cy3 or Alexa Fluor 633 (Jackson ImmunoResearch and Molecular Probes). The embryos were analyzed on a Zeiss LSM510 Meta laser scanning confocal microscope with Axiovision software and a Quorum spinning disc confocal microscope equipped with a Hamamatu C9100-13 EM-CCD and Volocity software. The objective lens used was 25× water, NA=0.80. Images were taken every 2.5-5 μm throughout the embryos.

In vitro mRNA transcription and microinjection
pCS2 Cre-NLS (Chazaud et al., 2006), pCS2 membrane-RFP (Megason and Fraser, 2004), pCS2 H2B-RFP and pCS2 Ezrin-GFP (Batchelor et al., 2004) were used in this study. In vitro transcription was performed using the mMESSAGE mMACHINE Sp6 Kit (Ambion). Synthesized mRNAs were dissolved in water and centrifuged in small capillaries to remove small debris before microinjection. Microinjection was performed as previously described (Chazaud et al., 2006).

Live imaging of preimplantation embryos
Time-lapse live imaging was performed on a Zeiss Axiovert inverted microscope equipped with Apotome and an environment controller. Embryos were placed on a glass-bottomed dish (MatTek) in KSOM covered with mineral oil. The objective lens used was 20× dry, NA=0.75. The camera used was an Axiocam MRm (1388×1044 pixels). For single eight-cell tracing, images were taken every 15 minutes with a 7-9 μm section interval (six *z*-sections/time point) for 24-30 hours. The typical experimental condition was: for DIC image acquisition, 2×2 binning, camera gain 0, exposure time 5 milliseconds and 2.4 V halogen light volume with NA=0.55 condenser setting; for RFP image acquisition, Cy3 filter, 2×2 binning, camera gain 3, exposure time 80 milliseconds and the minimum light volume (20%) of a mercury light source with further 90% of cutoff by a neutral density filter. Twelve embryos were imaged in single experiments. After image acquisition, the embryos were transferred individually to pseudo pregnant females (one embryo/single uterine horn). Embryos were recovered between embryonic day (E) 5.5 and E6.5 and the distribution of GFP expressing cells analyzed. No phototoxic effect was observed in this experimental condition as judged by a comparison of survival rates to term (control, 13 pups/24 transferred; imaged, 12 pups/25 transferred). To validate the accuracy of our positional live imaging tracing, one researcher scored cell position using live imaging of 28 embryos, which were then fixed following either the 8-16 or the 16-32 cell division. A second researcher counterstained each individual embryo with Par6 to visualize the apical membranes and independently scored cell position using the Quorum spinning disc confocal microscope with 1 μm sections (see Fig. S6 in the supplementary material). Both methods agreed with each other, confirming the accuracy of our experimental set-up. For *Pdgfra^H2B-GFP* mouse embryos, images were taken every 15-20 minutes with 6-7 μm section intervals (eight *z*-sections/time point) for 24-48 hours. The typical experimental condition

for GFP image acquisition was: FITC filter, 2×2 binning, camera gain 3, exposure time 250 milliseconds and the half-light volume (50%) of a mercury light source with further 50% of cutoff by a neutral density filter.

RESULTS
Live imaging analysis of generation of inner cells during two rounds of asymmetric divisions

We analyzed the generation of inner cells in intact embryos and examined the relationship between the developmental origins of ICM cells and their later cell fate. We combined both short- and long-term lineage analysis to trace the cleavage pattern of single eight-cell blastomeres and the cell fate of their progeny in later development. For short-term lineage analysis, we injected mRNA for histone H2B-RFP and membrane-RFP in which RFP is fused with a 2×Lyn membrane localization signal sequence (Megason and Fraser, 2003) to visualize the nuclei and cell shape, respectively. For long-term lineage analysis, we used the Z/EG mouse line (Novak et al., 2000), in which GFP expression is induced in cells after Cre

excision. To label single eight-cell blastomeres, mRNAs of the two RFP reporters and Cre recombinase were co-injected into one of the blastomeres in the eight-cell embryo. Thus, all progeny of single eight-cell blastomeres were permanently labeled with GFP, in addition to the short-term RFP labeling.

From studies of isolated blastomeres (reviewed by Johnson et al., 1986), it was suggested that there are two types of division at the 8-16 cell and 16-32 cell stages, symmetric and asymmetric. In the symmetric division, both daughter cells inherit an apical pole and form two outer, prospective TE cells. In the asymmetric division, only one of daughter cells inherits the apical pole and is maintained on the outside. The other forms an inner apolar and prospective ICM cell (Johnson and Ziomek, 1981). We observed 112 intact embryos from the eight-cell to the 32-cell stages, in which one of the blastomeres in the eight-cell embryo was labeled with the RFP reporters, and analyzed the initial positions of both daughter cells directly after cell division and their final outside or inside position within each cell cycle. We classified cell divisions generating outer
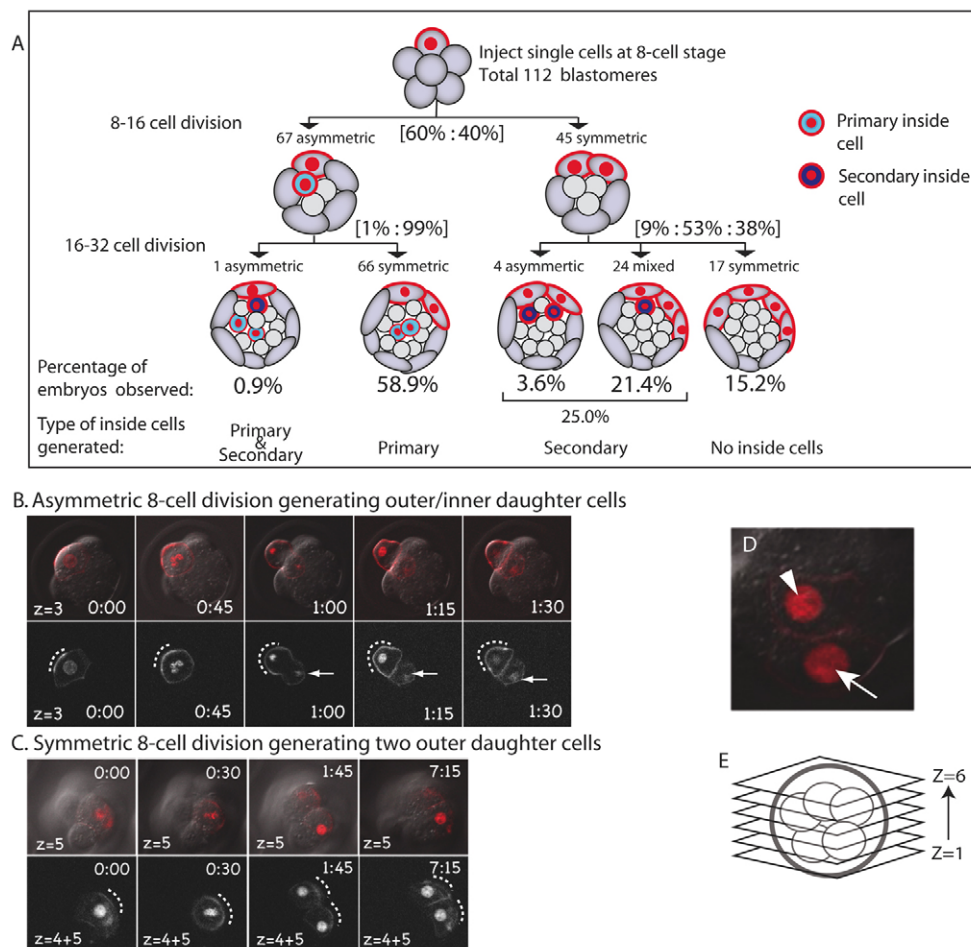

Fig. 1. Cell tracing analysis of single eight-cell blastomeres in intact mouse embryos. (**A**) Schematic of division patterns of single eight-cell blastomeres. A total of 112 embryos were observed from eight-cell to 32-cell stages. Numbers at the left side of arrows indicate the numbers of embryos observed in each category. Percentages in square brackets are the percentages of asymmetric/symmetric divisions in each category. (**B**) Asymmetric eight-cell division generated one outer and one inner cell. (t=0:00) An apical pole was observed as an enrichment of membrane-RFP (white dotted curves). (t=0:45) A dividing eight-cell blastomere. One of daughter cells (white arrows) was directly deposited inside of the embryo. (**C**) Symmetric eight-cell division generated two outer cells. (t=0:00) An apical enrichment of membrane-RFP was observed. (t=0:30) A dividing eight-cell blastomere. (t=1:45-7:15) Both daughter cells form outer cells. (**D**) Curved cell-cell contact between outer (white arrow) and inner (white arrowhead) cells. Color images show merged DIC and RFP channels. The black and white images are RFP channel only. Images were taken every 15 minutes with 6 z-sections/time point. The z-value indicates the optical section number from the bottom, as shown in the diagram in **E**.

and inner daughter cells as asymmetric (Fig. 1B; see also Movie 1 in the supplementary material), and ones generating two outer daughter cells as symmetric (Fig. 1C; see also Movie 2 in the supplementary material), based on the final allocation of cells within each cell cycle. Interestingly, in the majority of divisions classified as asymmetric, both 16-cell daughter blastomeres were initially positioned outside before one of the daughter cells was progressively internalized by surrounding outer cells to take up the internal position (see Fig. S1 and Movie 3 in the supplementary material).

In the 8-16 cell division, we found that 60% of labeled eight-cell blastomeres generated both outer and inner cells (Fig. 1A, 67 out of 112 eight-cell blastomeres) and 40% of them generated two outer cells (45 out of 112 eight-cell blastomeres). In the subsequent 16-32 cell division, 66 out of the 67 16-cell outer blastomeres generated by the previous asymmetric division generated two outside prospective TE cells (Fig. 1A). This suggested that these cells were strongly constrained to symmetric cell division. By contrast, 36% of the 16-cell outer blastomeres generated by the previous symmetric division were able to divide asymmetrically (Fig. 1A, 32 asymmetric divisions out of 90 16-32 cell blastomeres in the category). The frequency of asymmetrical division was lower than that observed in the previous 8-16 cell division.

Our aggregated data suggest that about 60% of eight-cell blastomeres (4.8 blastomeres in the eight-cell stage embryo) generated primary inner cells but only about 25% of them (two blastomeres in the eight-cell stage embryo) generated secondary inner cells (Fig. 1A). Because primary inner cells never generate outer cells, but do continue to divide from the 16- to 32-cell stage, this suggests that the early ICM at the 32-cell stage consists of approximately 9-10 cells derived from primary inner cells and no more than 2-3 secondary inner cells.

Cell fate analysis of primary and secondary inner cells

Next, we examined whether there was any difference in cell fate between primary and secondary inner cells. After tracing the cleavage pattern of single eight-cell blastomeres using the RFP signal, embryos were scored as having primary- or secondary-derived ICM cells and transferred individually to pseudo-pregnant females (one blastocyst/single uterine horn). Care was taken to ensure that GFP expression was only detected in the RFP-labeled progeny (see Fig. S2A,B in the supplementary material). Out of 91 transferred blastocysts, 66 embryos could be recovered between E5.5 and E6.5. The distribution of GFP cells was analyzed to determine the contribution of primary and secondary inner cells to EPI and/or PE lineages (see Fig. S2C in the supplementary material).

We found that neither primary nor secondary inner cells showed strict restriction towards one lineage (Table 1). The progeny of both primary and secondary inner cells were capable of contributing to both PE and EPI lineages. Some embryos, which had carried GFP-labeled ICM cells before transfer did not have any GFP-positive

cells in PE/EPI derivatives at E5.5-E6.5, suggesting that there was measurable cell death in the ICM during implantation, as reported previously (Copp, 1978; Plusa et al., 2008). Out of the surviving labeled progenies of the primary inner cells, 39% contributed to PE lineage only and 17% to EPI lineage only, whereas 25% contributed to both lineages (Table 1). The number of embryos in the secondary inner cell category is low, because of the smaller number of secondary inner cells in all embryos. However, the distribution of contributions was similar, with no restriction to either PE or EPI. We conclude that the developmental origins of the ICM cells from different cleavage divisions did not restrict the potential of the cells to generate either PE or EPI.

Treatment with specific FGF/MAP kinase signal inhibitors after the morula stage phenocopies the *Grb2* mutant

Previously our analysis of *Grb2* mutants showed that all ICM cells take up the Nanog-positive EPI progenitor state at E3.5 and fail to turn on Gata6 expression (Chazaud et al., 2006), suggesting a role for receptor tyrosine kinase signaling in PE formation. Indirect evidence implicated the FGF signaling pathway as the upstream pathway initiating PE fate through Grb2 (Arman et al., 1998; Feldman et al., 1995; Cheng et al., 1998). Here, we used a combination of an FGF receptor inhibitor, PD173074, and a MEK inhibitor, PD0325901 (Ying et al., 2008), to test the timing of requirement of the FGF/MAP kinase signal on PE formation.

When embryos were treated with both inhibitors from the eight-cell stage to late blastocyst stages, they showed a very similar phenotype to the *Grb2* mutant blastocyst (Chazaud et al., 2006). In control embryos, most ICM cells expressed either Nanog or Gata6 by the late blastocyst stage (Fig. 2C, part a; *n*=15). By contrast, all ICM cells strongly expressed Nanog and repressed Gata6 expression at E3.75 in the majority of inhibitor-treated embryos (seven out of 10 embryos; Fig. 2C, part b). The remaining embryos had only a few Gata6-positive cells remaining in the ICM. We counted the total number of ICM cells and found no significant difference between inhibitor-treated and control embryos (Fig. 2B). This suggested that those changes were due to neither selective proliferation nor apoptosis of one lineage, but to selective lineage choice, as we suggested in the *Grb2* mutant study (Chazaud et al., 2006).

Interestingly, embryos treated with inhibitors from the 8-16 cell to the early blastocyst stage and then replaced in control media showed no effects of the initial inhibitor treatment (Fig. 2C, part d; *n*=11). However, embryos treated with inhibitors after the early blastocyst stage showed the same upregulation of Nanog expression and downregulation of Gata6 expression in the ICM as the embryos treated with inhibitors from the eight-cell stage onwards (Fig. 2C, part c). This result suggested that activation of the FGF/MAP kinase signal after the early blastocyst stage is important for generation of the PE progenitors.

Table 1. Lineage contribution of primary and secondary inner cells in E5.5-E6.5 embryos

	Embryos with contribution to PE only	Embryos with contribution to PE and EPI	Embryos with contribution to EPI only	Embryos with no contribution to PE/EPI	Embryos recovered at E5.5-E6.5
Primary inner cells	17 (39)	11 (25)	6 (17)	10 (23)	44 (100)
Secondary inner cells	4 (30)	3 (23)	1 (8)	5 (39)	13 (100)
Primary and secondary	0	1	0	0	1
No inner cells	0	0	0	8	8
				23 (35)	66 (100)

Number of embryos in each category are shown. Numbers in parentheses indicate the percentages in recovered embryos.
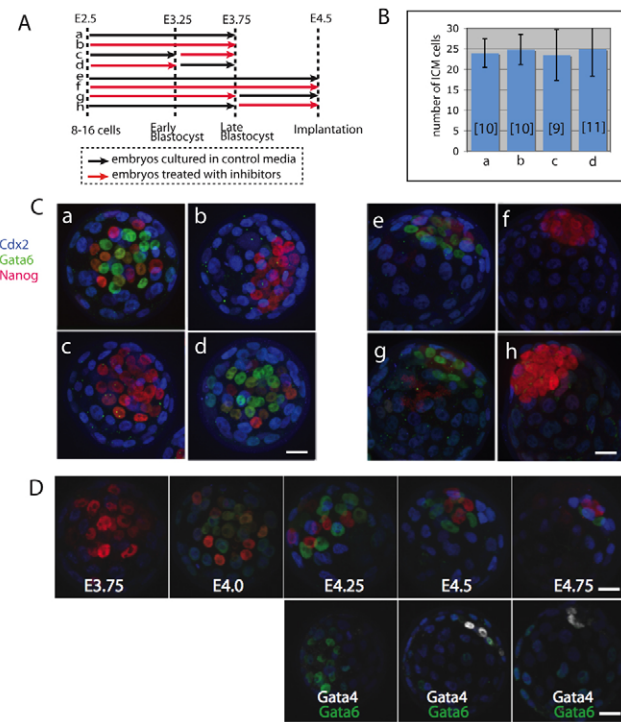
Fig. 2. Sustained inhibition of the FGF/MAP kinase signal is required to completely block PE formation. (**A**) Schematic of the time schedule of inhibitor treatment. Red and black arrows indicate the culture periods in the presence and absence of inhibitors, respectively. (**B**) Comparison of total ICM cell numbers at E3.75 in embryos cultured in the presence and absence of inhibitors. The number of embryos counted is shown in brackets. There was no statistically significant difference in ICM cell numbers in embryos cultured in different conditions. (**C**, parts a-d) E3.75 blastocysts cultured from E2.5 in the presence and absence of inhibitors. (C, part a) Control embryo. Gata6-positive PE progenitors and Nanog-positive EPI progenitors distributed randomly in the ICM. (C, part b) Embryo treated with inhibitors from E2.5-E3.75. All ICM cells became Nanog-positive EPI progenitors. (C, part c) Embryo initially cultured in control media and then treated with inhibitors. (C, part d) Embryo initially treated with inhibitors and then switched to control media. The embryo showed no difference to the control embryo. (C, parts e-h) E4.5 blastocysts cultured from E2.5 in the absence and presence of inhibitors. (C, part e) Control embryo. Nanog-positive EPI cells formed a cluster under the Gata6-positive PE layer. (C, part f) Embryo treated with inhibitors from E2.5 to E4.5. All ICM became Nanog-positive EPI. (C, part g) Embryo initially treated with inhibitors from E2.5 to E3.75 and then switched to control media. Gata6-positive PE cells were restored and forming a layer over an EPI cluster. (C, part h) Embryo initially cultured in control media from E2.5 to E3.75 and then treated with inhibitors. All E4.5 ICM cells became Nanog-positive EPI. (**D**) Embryos cultured with inhibitors of the FGF/MAP kinase signal from E2.5 to 3.75 then allowed to recover in the absence of the inhibitors. At E4.0, ICM cells began to co-express Nanog and Gata6 in a 'salt and pepper' manner. The PE cells subsequently formed a distinct layer. Gata4 expression was first detected at E4.5. Blue, Cdx2; green, Gata6; red, Nanog; white, Gata4. Scale bars: 20 µm.

Sustained inhibition of the FGF/MAP kinase signal in the blastocyst stage is essential to block PE formation

We then investigated whether Nanog-positive progenitors at E3.75 in the inhibitor-treated embryos were irreversibly restricted to the EPI state. To test this, we treated embryos with inhibitors till E3.75

and then released them from inhibitors (the time schedule of inhibitor-treatment is summarized in Fig. 2A). In embryos treated with inhibitors continuously from E2.5 to E4.5, all ICM cells became Nanog-positive EPI (Fig. 2C, part f; n=9). Surprisingly, embryos initially treated with inhibitors and then switched to control media as late as E3.75 regenerated Gata6-positive PE cells (Fig. 2C, part g; n=6). A Gata6-positive PE layer was formed on the outside of a cluster of Nanog-positive EPI similar to in untreated embryos. Similar results were obtained using a combination of FGFR/MEK/GSK3 inhibitors (see Fig. S3 in the supplementary material). This result suggested that, although all ICM cells became Nanog positive, Gata6 negative following inhibitor treatment, some of these cells were still capable of reverting to the PE phenotype.

We analyzed the time course of this reversion process (Fig. 2D) and found that Gata6 expression was restored in most ICM cells co-expressing Nanog within 6 hours of inhibitor removal, similar to the early blastocyst (Fig. 2D, E4.0). Subsequently, Nanog and Gata6 re-established the mutually exclusive expression pattern (Fig. 2D, E4.25) and the two lineages segregated to form distinct layers (Fig. 2D, E4.5). Similar to the progression of normal development (see Fig. S4 in the supplementary material), Gata4 expression was evident only subsequent to Gata6 expression (Fig. 2D).

We also examined the converse condition: the embryos were initially cultured in control media from E2.5 to E3.75, and then treated with inhibitors (Fig. 2C, part h; n=8). These embryos showed a similar phenotype to embryos treated continuously throughout this period: all ICM cells became Nanog-positive EPI and there were no Gata6-positive PE.

These results suggested that plasticity was still retained even after mutually exclusive Nanog or Gata6 expression is established. To examine when ICM cells lost this plasticity, embryos were removed from or treated with inhibitors at various time points after E3.75 and cultured for an additional 18 hours (Fig. 3A,B). In both experiments, plasticity was progressively lost after E4.0, indicating that lineage commitment to the EPI/PE lineage took place around E4.0-E4.5.

High level of FGF/MAP kinase signaling promotes PE formation

Our data suggested that sustained inhibition of the FGF/MAP kinase signal at the blastocyst stage is necessary to block PE formation completely. However, it is possible that the FGF/MAP kinase signal acts as a permissive signal but not an instructive one, with other signals being required to instruct PE fate. To address this, we investigated whether increasing the level of the FGF signal would be sufficient to produce a converse phenotype to the inhibitor-treated embryos, in which all ICM cells become Gata6-expressing PE progenitors.

We treated embryos with various doses of Fgf4 and heparin (1 µg/ml) continuously from E1.5 to E4.5 (the conditions are summarized in Fig. 4A). When embryos were treated with Fgf4 in doses higher than 250 ng/ml, we observed embryos in which all E4.5 ICM cells became Gata6-positive PE cells (Fig. 4C, part b; 500 ng/ml Fgf4 treated, n=28). The frequency of observing these embryos was clearly dose dependent (Fig. 4E). This phenotype was already apparent at E3.75 (Fig. 4B, part b). There were no statistically significant differences in the ICM cell number between control embryos and embryos treated with Fgf4 at E3.75 (Fig. 4D).

We examined whether sustained activation of the FGF/MAP kinase signal was required to block EPI and promote PE formation. When the effect of exogenous Fgf4 was interrupted with inhibitors after E3.25, Nanog-positive EPI progenitors were subsequently restored at E3.75 (Fig. 4B, part c). Although we wondered if the
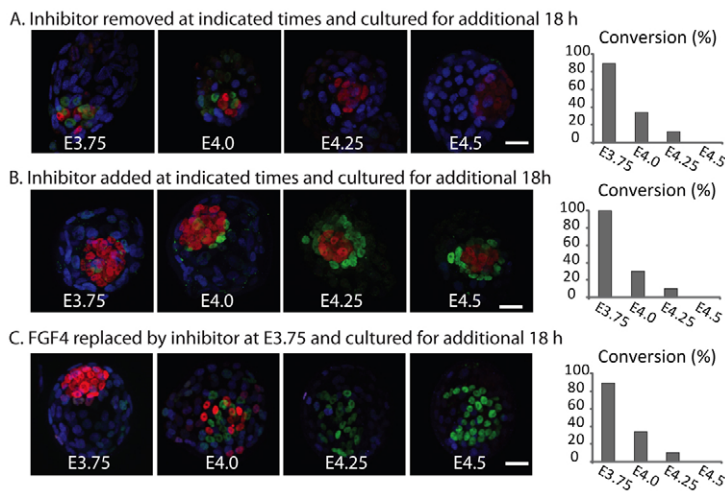
A. Inhibitor removed at indicated times and cultured for additional 18 h

B. Inhibitor added at indicated times and cultured for additional 18h

C. FGF4 replaced by inhibitor at E3.75 and cultured for additional 18 h

Fig. 3. Progressive loss of lineage plasticity in the ICM. (**A**) Embryos cultured with inhibitors from E2.5 and removed from the inhibitors at indicated time points. After an additional 18 hours culture in the control condition, the lineage conversion was examined. (**B**) Embryos were treated with inhibitors from the indicated time points and cultured for an additional 18 hours. (**C**) Embryos cultured with Fgf4 (500 ng/ml) and heparin, were treated with inhibitors from the indicated time points and cultured for additional 18 hour. Graphs on the right show the percentage of embryos with complete conversion. Blue, Cdx2; green, Gata6; red, Nanog. Scale bars: 20 μm.

exogenous Fgf4 treatment could induce the precocious commitment to the PE lineage, interruption of the treatment after E3.75 was also effective in restoring Nanog-positive EPI at E4.5 (Fig. 4C, part c). Similar to the previous inhibitor-removal/treatment experiments, the timing of lineage commitment was around E4.0-E4.5 (Fig. 3C). Consistent with this, exogenous FGF treatment after E3.75 was also effective in generating embryos in which all ICM cells became Gata6-positive PE (Fig. 4C, part d). Therefore, cells expressing either Nanog or Gata6 were able to respond to the activation level of the FGF/MAP kinase signaling level at all stages of blastocyst development until their final lineage commitment around E4.0-E4.5.

Live imaging analysis of the effects of altered FGF signaling

In order to observe the temporal aspects of the effects of altering FGF signaling on EPI versus PE specification, we performed live imaging using a PE-specific reporter line. The $Pdgfra^{H2B-GFP}$ mouse line is a useful PE reporter line in which to analyze the generation of heterogeneity in the E3.5 ICM and the process of sorting out of PE and EPI progenitors (Plusa et al., 2008). As a control, we first analyzed GFP expression in $Pdgfra^{H2B-GFP/+}$ embryos cultured in control medium (n=3). At around E3.35 (Fig. 5A, t=0:00; see also Movie 4 in the supplementary material), we could not observe GFP under our experimental conditions, probably because of the limited exposure to the excitation light used to reduce the phototoxicity to the embryos, although expression of GFP was detected in a previous study (Plusa et al., 2008). When the excitation light was enhanced, we did detect GFP (data not shown). Slightly after E3.5, weak expression was detected in the majority of ICM cells (t=6:15). Some ICM cells began to express higher GFP after around E3.75 (t=12:00 in Fig. 5A). Around E4.0 (t=18:15), a morphologically distinct GFP-positive PE layer was observed, although a few GFP-positive cells were still in the deep position. These observations were consistent with those of the previous study (Plusa et al., 2008).

Next, we treated $Pdgfra^{H2B-GFP/+}$ embryos with the FGFR/MEK inhibitors after E3.75 (Fig. 5B, see Movie 5 in the supplementary material). At E3.75, GFP expression was observed in some of the ICM cells, similar to in the control embryo (Fig. 5B; t=0:00). Inhibitor treatment prevented the increased intensity and expansion of GFP expression that was seen in the controls, although the initial expression in a few cells was maintained. Furthermore, instead of forming a morphologically visible PE layer, those lingering GFP-positive cells remained scattered in the ICM (Fig. 5B; t=24:00). We

confirmed that Gata6 expression was not detectable and that Nanog expression was upregulated in all ICM cells in these inhibitor-treated embryos (see Fig. S5 in the supplementary material). The residual GFP expression was presumably due to the relatively long half-life of H2B-GFP. When $Pdgfra^{H2B-GFP/+}$ embryos were treated with high-dose Fgf4 (500 ng/ml, n=3) from the 2- to 4-cell stage, GFP expression was readily detected in the early blastocyst stage (Fig. 5C; t=0:00; see Movie 6 in the supplementary material). GFP expression consistently appeared higher than in the $Pdgfra^{H2B-GFP/+}$ embryos cultured in control media and the majority of ICM cells were GFP positive (Fig. 5C, t=10:00). These GFP-positive ICM cells maintained GFP expression at a high level and no GFP-negative cells were observed in the ICM (Fig. 5C; t=16:15-30:00). There was some cell death observed by the end of the observation period (Fig. 5C; t=30:00). These movies confirmed that the cell fate shift in the ICM to either EPI or PE by inhibition of FGF signaling or addition of exogenous FGF is due to the transformation of individual progenitor cells to the alternative lineage, without selective apoptosis or proliferation.

Taken together, E3.5 ICM cells are instructed towards the EPI or PE fate in a FGF/MAP kinase signal-dependent manner. The expression of Nanog and Gata6 is likely to reflect the activation level of the FGF/MAP kinase signal in individual ICM cells during maturation of the blastocyst. Those progenitors progressively commit to the EPI or PE fate but, during the transition, they are still sensitive to the balance of the FGF/MAP kinase signaling levels.

DISCUSSION
The generation of enclosed inside cells is the first important step towards forming distinct lineages in the early mouse embryo. Here, we follow these events in living embryos and provide a quantitative analysis of the likelihood of individual blastomeres at the eight- and 16-cell stage generating inner or outer cells at each division. This process was previously analyzed in the 1980s using isolated blastomeres, and two important cellular events were discovered: polarization in eight-cell blastomeres, and the two types of division at the 8-16 cell division – symmetric and asymmetric (Johnson and Ziomek, 1981) (reviewed by Johnson et al., 1986). In experiments using isolated eight-cell blastomeres, the frequency to divide asymmetrically was around 82-85 %. By contrast, when eight-cell blastomeres were paired with others, the frequency was changed to around 50% (Pickering et al., 1988). This suggested that cell-cell contact was somehow affecting the outcome of divisions. However,

Fig. 4. High-dose Fgf4 treatment is sufficient to block EPI formation.
(**A**) Schematic of the time schedule of FGF treatment. Black and red arrows indicate the culture periods in the absence and presence of the FGFR/MEK inhibitors, respectively. Blue arrows indicate the culture periods in the presence of Fgf4 and heparin. (**B**) E3.75 blastocysts treated with or without exogenous Fgf4 and heparin. (B, part a) Control embryo cultured from E1.5 in control media. (B, part b) Embryo treated with Fgf4 (500 ng/ml) and heparin. All ICM cells downregulated Nanog expression and became Gata6-positive PE progenitors. (B, part c) Embryo initially treated with Fgf4 (500 ng/ml) and heparin, and then switched to the presence of the FGFR/MEK inhibitors. The effect of exogenous Fgf4 was completely blocked and most of the ICM cells were Nanog-positive EPI progenitors. (**C**) E4.5 blastocysts. (C, part a) Control embryo. Nanog-positive EPI formed a cluster under a monolayer of Gata6-positive PE. (C, part b) Embryo treated with Fgf4 (500 ng/ml) and heparin. All E4.5 ICM cells became Gata6-positive PE cells. (C, part c) Embryo initially treated with Fgf4 (500 ng/ml) and heparin until E3.75 and then treated with inhibitors. The effect of exogenous Fgf4 was blocked and most E4.5 ICM cells became Nanog-positive EPI cells. (C, part d) Embryo initially treated with inhibitors until E3.75 and then switched to treatment with Fgf4 (500 ng/ml) and heparin until E4.5. Blue, Cdx2; green, Gata6; red, Nanog. Scale bars: 20 μm. (**D**) Comparison of total ICM cell numbers at E3.75 in embryos treated with or without Fgf4. The number of counted embryos is shown in brackets. There was no statistically significant difference in number of ICM cells in embryos cultured in different conditions. (**E**) Fgf4 dose-dependent generation of all PE ICM embryos at E4.5. More than 10 embryos were scored at each dose point. Embryos treated with high-dose of Fgf4 (>250 ng/ml) generated the E4.5 ICM without any EPI cells.
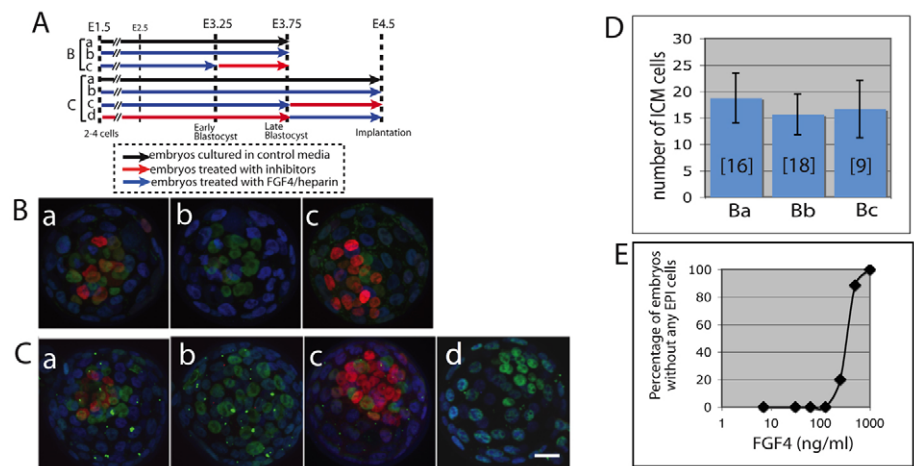
none of these studies were performed in intact embryos because of technical limitations at that time. Fleming counted inner and outer cells in 16-cell morulae (Fleming, 1987) and observed considerable variation among embryos (the ratio of outer:inner cells ranged from 9:7 to 14:2), but the average outer:inner cell ratio was 10.8:5.2. Merging these results suggested that 65% of eight-cell blastomeres divide asymmetrically, the intermediate frequency between isolated and paired blastomeres. This frequency is comparable to the frequency we observed in our direct lineage-tracing experiment (Fig. 1A, 60% of eight-cell blastomeres divided asymmetrically). Although Fleming hypothesized that the embryo has mechanisms in the next cell division (16-32) to compensate for the considerable variation of the outer:inner cell ratio in the 16-cell stage, our results suggest that the variation he observed might be due to the timing of scoring for cell position and asymmetric division. As we show in Fig. S1 in the supplementary material, not all of the 16-cell stage inner cells were allocated inside soon after division. Most inner cells were initially located outside (58 out of 67 inner cells) and then progressively internalized. This may cause over-representation of outer cells after the 8-16 cell division, if outer cells were counted based solely on the presence of surface label. By following individual eight-cell blastomeres from the eight-cell to the blastocyst stage, we were able to directly score the outcome of each division. A division may initially appear to be symmetric as two daughter cells localize outside, but subsequent, probably intrinsically controlled, cell movement can regulate their final functional allocation in the embryo without the compensatory mechanisms. These results suggest that revisiting classic data with modern cell tracing techniques in intact embryos is important to verify whether our current knowledge is correct in normal intact development.

Interestingly, 16-cell stage outer cells generated from previous asymmetric divisions showed strong constraint towards symmetric divisions at the next division (Fig. 1A; 66 out of 67 16-32 outer cell

divisions). This is similar to the 100% symmetric division of 16-cell stage polar cells paired with 16-cell stage apolar cells (Johnson and Ziomek, 1983). Conversely, 16-cell stage outer cells generated from previous symmetric divisions showed a 36% frequency of asymmetric divisions (Fig. 1A; 32 out of the 90 16-32 outer cell division in the category). This is an intermediate frequency of asymmetric divisions between those observed in isolated single 16-cell stage polar cells and two paired 16-cell stage polar cells, 48% and 14%, respectively (Johnson and Ziomek, 1983). The reason for this difference is not clear but it has major impact on the lineage tree of ICM cells (Fig. 1A). The number of cell-cell contacts, history of cell division and/or shape of cells seem to be factors in regulating the divisional orientation. Further investigation will be required to understand the molecular mechanisms that regulate divisional orientation in the preimplantation embryo.

Interestingly, inner, presumed apolar cells intrinsically take up the inner position, regardless of their initial position after cleavage division. We noticed that the cell-cell contact between inner and outer cells is often curved towards the polar side (Fig. 1D), although the contact between two outer cells or two inner cells is usually flat. This phenomenon has already been reported from experiments using isolated blastomeres: apolar cells are engulfed by polar cells and the cell-cell contact is curved towards polar cells between the two populations (Johnson and Ziomek, 1983). These results suggested that inner cells have a higher cortical tension than outer cells. It has been shown that cortical tension plays an important role in sorting out different cell populations, in addition to adhesion differences (Krieg et al., 2008). Cells having higher cortical tension occupy the inner space in cell aggregates. The configuration of polar and apolar cells matches this model. In the mouse embryo, cell adhesion, mediated by E-cadherin, is essential for compaction (De Vries et al., 2004; Larue et al., 1994; Shirayoshi et al., 1983), but there is no evidence of differential adhesion between inner and outer cells. Thus, we suggest that the difference in cortical tension
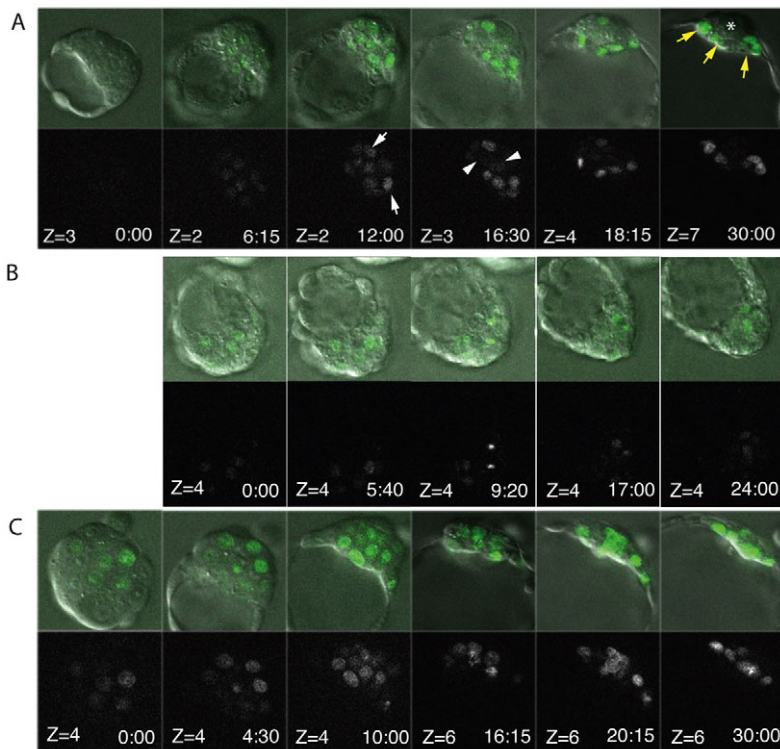
DEVELOPMENT

Fig. 5. Live imaging analysis of PE formation in the Pdgfra^H2B-GFP mouse line. (**A**) Pdgfra^H2B-GFP/+ embryo in control culture medium. (t=0:00) The early blastocyst stage, at E3.3. (t=6:15) A weak GFP signal was detected in a majority of ICM cells. (t=12:00-14:00) Some ICM cells showed a higher GFP signal (white arrows) and GFP-negative cells were also observed (white arrowheads). (t=18:15-30:00) GFP-positive PE cells were forming a morphologically distinct layer (yellow arrows) on a cluster of EPI cells (white asterisks). (**B**) Pdgfra^H2B-GFP/+ embryo treated with inhibitors after E3.7. (t=0:00) Some ICM cells expressed GFP. (t=9:20-24:00) Instead of forming a surface PE layer, GFP-positive cells were scattered in the ICM. (**C**) Pdgfra^H2B-GFP/+ embryo in the presence of Fgf4 (500 ng/ml) and heparin. The embryo was cultured in the presence of Fgf4 from E1.5. (t=0:00) Some ICM cells already expressed a detectable level of GFP at E3.3. (t=4:30-16:15) The majority of ICM cells expressed and maintained high GFP expression. (t=16:15-30:00) ICM cells became GFP-positive PE cells. Color images show merged DIC and GFP channels. The black and white images show the GFP channel only. Images were taken every 15 minutes (A and C) or 20 minutes (B) with eight z-sections/time point. The z-value indicates the optical section number from the bottom. Each time point is shown as hours:minutes.

between polar and apolar cells after the 8-16 cell division plays a key role in allocating cells to the outside and inside environment, respectively.

Our data showed that most eight-cell blastomeres generate either primary or secondary inner cells but rarely both. It is very rare for a polar cell derived from an asymmetric division of an eight-cell blastomere to undergo an asymmetric division at the next cleavage. We also clearly showed that the majority of early ICM cells are primary inner cell derived and only a few are secondary derived. We did not find any difference in postimplantation lineage contribution from progenies of primary or secondary inner cells. Thus, the process of generating a primary or secondary inner cell is not, in itself, sufficient to restrict later cell fate. Indeed, the observed ratio of approximately 9-10 cells derived from primary inner cells, and only 2-3 secondary inner cells is difficult to reconcile with the roughly equivalent numbers of Nanog-positive EPI progenitors and Gata6-positive PE progenitors observed in the ICM.

Our data do, however, indicate that regulation of the FGF/MAP kinase signal level at the blastocyst stage is essential and sufficient for segregation of these two lineages. Importantly, we show that blocking FGF/MAP kinase signaling promotes EPI cell fate and excess FGF promotes PE fate. Furthermore, the responsiveness of ICM cells to altered levels of FGF signaling continues beyond the time of first appearance of mosaic expression of EPI and PE markers at the E3.5 blastocyst stage.

So how is the apparently random 'salt and pepper' distribution of Gata6 and Nanog-expressing progenitors generated in the ICM? We propose that it happens in a stochastic manner dependent on the level of the FGF/MAP kinase signal (Fig. 6). As we have shown here, complete block of this signal leads all ICM cells to become Nanog positive, whereas high levels of the signal, to the contrary, leads all ICM cells to become Gata6 positive. At intermediate levels of activation (e.g. likely endogenous levels in

normal embryos), individual ICM cells would stochastically or probabilistically respond to the signal. The level of signal controls the proportion of cells able to respond but not the spatial distribution of those cells. Intrinsic and extrinsic variations (noise) in individual cells determine whether cells can respond to the signal (Nijhout, 2004; Raj and van Oudenaarden, 2008; Huang, 2009). It is still possible that the position within the ICM and/or the other signal(s) could create preference in cell fate by modulating the intra- and extra-cellular response the FGF/MAP kinase signal (Meilhac et al., 2009). It is known from single ICM cell transcriptome studies that there is intrinsic variation in the levels of expression of Fgf4 and Fgfr2 among the cells of the ICM (Kurimoto et al., 2006). The balance between Nanog and Gata6 seems to be regulated by the probabilistic response to the FGF/MAP kinase signal in individual ICM cells.

It was recently reported that combined inhibition of FGFR/ERK/GSK3 signaling also blocked PE differentiation (Nichols et al., 2009), similar to the *Grb2* mutant phenotype (Chazaud et al., 2006). Our detailed analysis revealed a dynamic plasticity in ICM cells even after cells had established exclusive Nanog or Gata6 expression. This plasticity progressively declined and was ultimately lost by E4.5. Gata4 might be a key player in the restriction of PE cell fate. Gata4 expression follows Gata6 expression and rarely overlaps with Nanog expression (Plusa et al., 2008). Establishment of a positive self-reinforcing regulatory circuit between Gata6 and Gata4 would allow cells to be released from the FGF/MAP kinase signal dependency and to commit to the PE lineage (Fujikura et al., 2002; Plusa et al., 2008).

There are some interesting similarities and differences between the response of ICM and ES cells to changes in levels of FGF signaling. It has been shown that Nanog expression fluctuates in ES cells in conventional ES culture conditions (Chambers et al., 2007; Singh et al., 2007). This fluctuation has been suggested to be
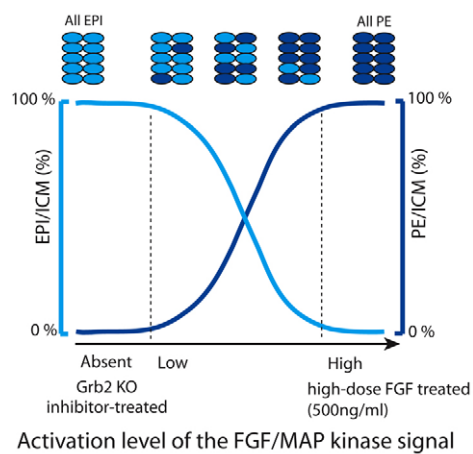
Fig. 6. Schematic model for FGF/MAP kinase signal dependent stochastic determination of PE and EPI lineages. The *x*-axis indicates the presumptive activation level of the FGF/MAP kinase signal. The *y*-axis indicates the proportion of the EPI (light blue) and PE (dark blue) in the ICM. When the signal is absent (e.g. in the ICM in *Grb2* mutants or in embryos treated with the FGFR/MEK inhibitors), all ICM cells take up the EPI fate. On the contrary, when the signal is high (e.g. in the ICM in embryos treated with high-dose of Fgf4), all ICM cells take up the PE fate. At the intermediate level of activation, individual ICM cells stochastically respond to the FGF/MAP kinase signal. The proportion of the two lineages is controlled as the proportion of FGF/MAP kinase signal activated cells. However, the distribution of the two lineages is unpredictable and random.

important for the balance between maintenance of pluripotency and priming for differentiation (Chambers et al., 2007; Kunath et al., 2007). Loss of Fgf4 arrests differentiation of ES cells (Kunath et al., 2007), and inhibition of FGF signaling with pharmacological inhibitors blocks the fluctuation and maintains stable *Nanog* expression in ES cells (Lanner et al., 2009). Forced activation of the MAP kinase pathway is sufficient to induce PE differentiation in ES cells without EB formation (Hamazaki et al., 2006). In contrast to our data showing that exogenous FGF induces ectopic PE in the blastocyst, exogenous FGF fails to enhance PE differentiation in EBs (Hamazaki et al., 2006). The FGF/MAP kinase signal in ES cells must be tightly controlled to prevent spontaneous PE differentiation.

It is interesting to note that treatment of embryos with the FGFR/MEK inhibitors did not alter cell fate in the trophectoderm: no upregulation of Nanog or loss of Cdx2 expression was observed, although it is known that FGF is required for trophoblast stem cell maintenance and proliferation (Tanaka et al., 1998). The endogenous source of FGF that promotes both PE cell fate and trophoblast stem cell proliferation is almost certainly Fgf4, which is produced by the developing ICM in direct response to Oct4/Sox2 regulation (Nichols et al., 1998; Yuan et al., 1995). Thus, the same source of FGF signal can produce different responses in outer trophectoderm or inner cell mass progenitors. The outside and inside cells of the blastocyst have experienced different levels of at least one other signaling pathway, the Hippo signaling pathway (Nishioka et al., 2009), suggesting that cell signaling history might lead to differential responses to FGF signals at the blastocyst stage. FGF signaling has multiple roles and initiates different responses in blastocyst cells depending on their history of exposure to different signaling pathways during development.

It is known that the preimplantation mouse embryo is highly plastic and resistant to various experimental perturbations. Stochastic gene regulation, evolving signaling environments and subsequent self-organization processes (positive- and negative-feedback networks) during the morula to blastocyst stage allows robust reproducibility of establishment of the three first lineages in the embryo without the necessity for any stereotypical early development.

References
Arman, E., Haffner-Krausz, R., Chen, Y., Heath, J. K. and Lonai, P. (1998). Targeted disruption of fibroblast growth factor (FGF) receptor 2 suggests a role for FGF signaling in pregastrulation mammalian development. *Proc. Natl. Acad. Sci. USA* **95**, 5082-5087.
Avner, P. and Heard, E. (2001). X-chromosome inactivation: counting, choice and initiation. *Nat. Rev. Genet.* **2**, 59-67.
Batchelor, C. L., Woodward, A. M. and Crouch, D. H. (2004). Nuclear ERM (ezrin, radixin, moesin) proteins: regulation by cell dencity and nuclear import. *Exp. Cell Res.* **296**, 208-222.
Chambers, I., Silva, J., Colby, D., Nichols, J., Nijmeijer, B., Robertson, M., Vrana, J., Jones, K., Grotewold, L. and Smith, A. (2007). Nanog safeguards pluripotency and mediates germline development. *Nature* **450**, 1230-1234.
Chazaud, C., Yamanaka, Y., Pawson, T. and Rossant, J. (2006). Early lineage segregation between epiblast and primitive endoderm in mouse blastocysts through the Grb2-MAPK pathway. *Dev. Cell* **10**, 615-624.
Chen, Y., Li, X., Eswarakumar, V. P., Seger, R. and Lonai, P. (2000). Fibroblast growth factor (FGF) signaling through PI 3-kinase and Akt/PKB is required for embryoid body differentiation. *Oncogene* **19**, 3750-3756.
Cheng, A. M., Saxton, T. M., Sakai, R., Kulkarni, S., Mbamalu, G., Vogel, W., Tortorice, C. G., Cardiff, R. D., Cross, J. C., Muller, W. J. et al. (1998). Mammalian Grb2 regulates multiple steps in embryonic development and malignant transformation. *Cell* **95**, 793-803.
Chisholm, J. C. and Houliston, E. (1987). Cytokeratin filament assembly in the preimplantation mouse embryo. *Development* **101**, 565-582.
Copp, A. J. (1978). Interaction between inner cell mass and trophectoderm of the mouse blastocyst. I. A study of cellular proliferation. *J. Embryol. Exp. Morphol.* **48**, 109-125.
De Vries, W. N., Evsikov, A. V., Haac, B. E., Fancher, K. S., Holbrook, A. E., Kemler, R., Solter, D. and Knowles, B. B. (2004). Maternal beta-catenin and E-cadherin in mouse development. *Development* **131**, 4435-4445.
Feldman, B., Poueymirou, W., Papaioannou, V. E., DeChiara, T. M. and Goldfarb, M. (1995). Requirement of FGF-4 for postimplantation mouse development. *Science* **267**, 246-249.
Fleming, T. P. (1987). A quantitative analysis of cell allocation to trophectoderm and inner cell mass in the mouse blastocyst. *Dev. Biol.* **119**, 520-531.
Fujikura, J., Yamato, E., Yonemura, S., Hosoda, K., Masui, S., Nakao, K., Miyazaki, Ji. J. and Niwa, H. (2002). Differentiation of embryonic stem cells is induced by GATA factors. *Genes Dev.* **16**, 784-789.
Gardner, R. L. (1982). Investigation of cell lineage and differentiation in the extraembryonic endoderm of the mouse embryo. *J. Embryol. Exp. Morphol.* **68**, 175-198.
Gardner, R. L. (1984). An in situ cell marker for clonal analysis of development of the extraembryonic endoderm in the mouse. *J. Embryol. Exp. Morphol.* **80**, 251-288.
Gardner, R. L. and Papaioannou, V. E. (1975). Differentiation in the trophectoderm and inner cell mass. In *The Early Develpment of Mammals* (ed. M. Balls and A. E. Wild), pp. 107-132. Cambridge: Cambridge University Press.
Gardner, R. L. and Rossant, J. (1979). Investigation of the fate of 4-5 day post-coitum mouse inner cell mass cells by blastocyst injection. *J. Embryol. Exp. Morphol.* **52**, 141-152.
Goldin, S. N. and Papaioannou, V. E. (2003). Paracrine action of FGF4 during periimplantation development maintains trophectoderm and primitive endoderm. *Genesis* **36**, 40-47.

Hamazaki, T., Kehoe, S. M., Nakano, T. and Terada, N. (2006). The Grb2/Mek pathway represses Nanog in murine embryonic stem cells. *Mol. Cell. Biol.* **26**, 7539-7549.

Huang, S. (2009). Non-genetic heterogeneity of cells in development: more than just noise. *Development* **136**, 3853-3862.

Johnson, M. H. and Ziomek, C. A. (1981). The foundation of two distinct cell lineages within the mouse morula. *Cell* **24**, 71-80.

Johnson, M. H. and Ziomek, C. A. (1983). Cell interactions influence the fate of mouse blastomeres undergoing the transition from the 16- to 32-cell stage. *Dev. Biol.* **95**, 211-218.

Johnson, M. H., Chisholm, J. C., Fleming, T. P. and Houliston, E. (1986). A role for cytoplasmic determinants in the development of the mouse early embryo? *J. Embryol. Exp. Morphol.* **97**, 97-121.

Krieg, M., Arboleda-Estudillo, Y., Puech, P. H., Kafer, J., Graner, F., Muller, D. J. and Heisenberg, C. P. (2008). Tensile forces govern germ-layer organization in zebrafish. *Nat. Cell. Biol.* **10**, 429-436.

Kunath, T., Saba-El-Leil, M. K., Almousailleakh, M., Wray, J., Meloche, S. and Smith, A. (2007). FGF stimulation of the Erk1/2 signalling cascade triggers transition of pluripotent embryonic stem cells from self-renewal to lineage commitment. *Development* **134**, 2895-2902.

Kurimoto, K., Yabuta, Y., Ohinata, Y., Ono, Y., Uno, K. D., Yamada, R. G., Ueda, H. R. and Saitou, M. (2006). An improved single-cell cDNA amplification method for efficient high-density oligonucleotide microarray analysis. *Nucleic Acids Res.* **34**, e42.

Lanner, F., Lee, K. L., Sohl, M., Holmborn, K., Yang, H., Wilbertz, J., Poellinger, L., Rossant, J. and Farnebo, F. (2009). Heparan sulfation dependent FGF signalling maintains embryonic stem cells primed for differentiation in a heterogeneous state. *Stem Cells* (e-pub ahead of print).

Larue, L., Ohsugi, M., Hirchenhain, J. and Kemler, R. (1994). E-cadherin null mutant embryos fail to form a trophectoderm epithelium. *Proc. Natl. Acad. Sci. USA* **91**, 8263-8267.

Megason, S. G. and Fraser, S. E. (2003). Digitizing life at the level of the cell: high-performance laser-scanning microscopy and image analysis for in toto imaging of development. *Mech. Dev.* **120**, 1407-1420.

Meilhac, S. M., Adams, R. J., Morris, S. A., Danckaert, A., Le Garrec, J. F. and Zernicka-Goetz, M. (2009). Active cell movements coupled to positional induction are involved in lineage segregation in the mouse blastocyst. *Dev. Biol.* **331**, 210-221.

Nichols, J., Zevnik, B., Anastassiadis, K., Niwa, H., Klewe-Nebenius, D., Chambers, I., Scholer, H. and Smith, A. (1998). Formation of pluripotent stem cells in the mammalian embryo depends on the POU transcription factor Oct4. *Cell* **95**, 379-391.

Nichols, J., Silva, J., Roode, M. and Smith, A. (2009). Supression of Erk signaling promotes ground state pluripotency in the mouse embryo. *Development* **136**, 3215-3222.

Nijhout, H. F. (2004). Statistic gene expression: dominance, thresholds and boundaries. In *The Biology of Genetic Dominance* (ed. R. A. Veitia). Eurekah.com., Chapter 8, 1-15.

Nishioka, N., Inoue, K., Adachi, K., Kiyonari, H., Ota, M., Ralston, A., Yabuta, N., Hirahara, S., Stephenson, R. O., Ogonuki, N. et al. (2009). The Hippo signaling pathway components Lats and Yap pattern Tead4 activity to distinguish mouse trophectoderm from inner cell mass. *Dev. Cell* **16**, 398-410.

Novak, A., Guo, C., Yang, W., Nagy, A. and Lobe, C. G. (2000). Z/EG, a double reporter mouse line that expresses enhanced green fluorescent protein upon Cre-mediated excision. *Genesis* **28**, 147-155.

Pickering, S. J., Maro, B., Johnson, M. H. and Skepper, J. N. (1988). The influence of cell contact on the division of mouse 8-cell blastomeres. *Development* **103**, 353-363.

Plusa, B., Piliszek, A., Frankenberg, S., Artus, J. and Hadjantonakis, A. K. (2008). Distinct sequential cell behaviours direct primitive endoderm formation in the mouse blastocyst. *Development* **135**, 3081-3091.

Raj, A. and van Oudenaarden, A. (2008). Nature, nurture, or chance: stochastic gene expression and its consequences. *Cell* **135**, 216-226.

Rappolee, D. A., Basilico, C., Patel, Y. and Werb, Z. (1994). Expression and function of FGF-4 in peri-implantation development in mouse embryos. *Development* **120**, 2259-2269.

Rossant, J. (1975). Investigation of the determinative state of the mouse inner cell mass. II. The fate of isolated inner cell masses transferred to the oviduct. *J. Embryol. Exp. Morphol.* **33**, 991-1001.

Rossant, J. and Tam, P. P. (2009). Blastocyst lineage formation, early embryonic asymmetries and axis patterning in the mouse. *Development* **136**, 701-713.

Shirayoshi, Y., Okada, T. S. and Takeichi, M. (1983). The calcium-dependent cell-cell adhesion system regulates inner cell mass formation and cell surface polarization in early mouse development. *Cell* **35**, 631-638.

Singh, A. M., Hamazaki, T., Hankowski, K. E. and Terada, N. (2007). A heterogeneous expression pattern for Nanog in embryonic stem cells. *Stem Cells* **25**, 2534-2542.

Tanaka, S., Kunath, T., Hadjantonakis, A. K., Nagy, A. and Rossant, J. (1998). Promotion of trophoblast stem cell proliferation by FGF4. *Science* **282**, 2072-2075.

Yamanaka, Y., Ralston, A., Stephenson, R. O. and Rossant, J. (2006). Cell and molecular regulation of the mouse blastocyst. *Dev. Dyn.* **235**, 2301-2314.

Ying, Q. L., Wray, J., Nichols, J., Batlle-Morera, L., Doble, B., Woodgett, J., Cohen, P. and Smith, A. (2008). The ground state of embryonic stem cell self-renewal. *Nature* **453**, 519-523.

Yuan, H., Corbi, N., Basilico, C. and Dailey, L. (1995). Developmental-specific activity of the FGF-4 enhancer requires the synergistic action of Sox2 and Oct-3. *Genes Dev.* **9**, 2635-2645.